sciendo

POLISH MARITIME RESEARCH 3 (123) 2024 Vol. 31; pp. 126-134
10.2478/pomr-2024-0042

Active Diagnostic Experimentation on Wind Turbine Blades with Vibration Measurements and Analysis

Zbigniew Korczewski *
Jacek Rudnicki
Gdańsk University of Technology, Poland

* Corresponding author: *zbikorcz@pg.edu.pl (Z. Korczewski)*

ABSTRACT

This paper deals with the key operational problems of wind turbosets, especially offshore, where vibrations are generated by rotor blades, as a consequence of erosive wear or icing. The primary causes of the imbalance of wind turbine rotors have been characterised, the observable symptoms of which include various forms of vibrations, transmitted from the turbine wheel to the bearing nodes of the power train components. Their identification was the result of an active diagnostic experiment, which actually entered the aerodynamic-mass imbalance of a turbine rotor into a wind power train, built as a small scale model. The recording of the observed monitoring parameters (vibration, aerodynamic, mechanical and electrical) made it possible to determine a set of symptoms (syndrome) of the deteriorated (entered) dynamic state of the entire wind turboset. This provides the basis for positive verification of the assumed concept and methodology of diagnostic testing, the constructed laboratory station and the measuring equipment used. For this reason, testing continued, taking into account the known and recognisable faults that most often occur during the operation of offshore wind turbosets. Transferring the results of this type of model research to full-size, real objects makes it possible to detect secondary (fatigue) damage to the elements transmitting torque from the wind turbine rotor to the generator early, especially the thrust bearings or gear wheel teeth.

Keywords: offshore wind turbine blades, vibration-based health monitoring, active experimentation

INTRODUCTION

Modern offshore wind turbosets are characterised by high power (up to 15 MW), huge dimensions (turbine rotors with diameters over 200 m, installed at a height of approximately 150 m) and weight (over 1,000 tons), which results from the need to optimally match the dimensions of the turbines to the available wind energy[1], in order to reduce investment costs[2] [2]. The operation of wind turbosets in ocean conditions requires a number of specific actions from the user, which determine the possibility of achieving the maximum design power and the efficiency of the implemented energy processes, while maintaining high

1 Winds blowing at sea are much stronger and more steady than those blowing over land. For this reason, on the one hand, a rational investment action is to adequately increase the dimensions of the turbine rotor, in order to maximise the harvesting kinetic energy of the wind. On the other hand, it requires appropriate strengthening of the supporting structure.

2 It is estimated that the investment cost of an offshore wind farm is 1.4-2.0 million Euro per 1 MW of power, while the annual costs of usage and servicing is 30-50 thousand euro per 1 MW of power [7].

operational reliability and durability (usually defined as 25 years) [8]. A characteristic feature of the usage process of this type of power system is the need to ensure continuous operation[3] under variable load conditions and the simultaneous destructive impact of the sea-operating environment, which consequently favours the generation of faults. Additionally, this takes place in the absence of direct operator supervision and significantly limited accessibility to the wind turbosets used; they are located at sea, at a distance of 30-40 km (or more) from the coastline. However, planned and ad hoc maintenance activities, including diagnostics, are determined by broadly understood weather conditions (wind strength, sea state, atmospheric phenomena, etc.). It is true that the larger the wind turbines are, the lower the costs of standard maintenance activities on wind turbosets (converted to generate power), which are estimated to be at a level of 20-25%[4] of the total income from electricity generated in offshore wind farms [16]. In turn, the costs of the so-called 'emergency services' resulting from sudden damage to offshore wind turbosets increase dramatically along with their power and age. For the above reasons, a key operational problem is the early recognition of symptoms (syndromes) of slowly developing primary faults in the most critical components. The results of statistical testing prove that such components include wind turbine rotor blades, see Fig. 1 [18].

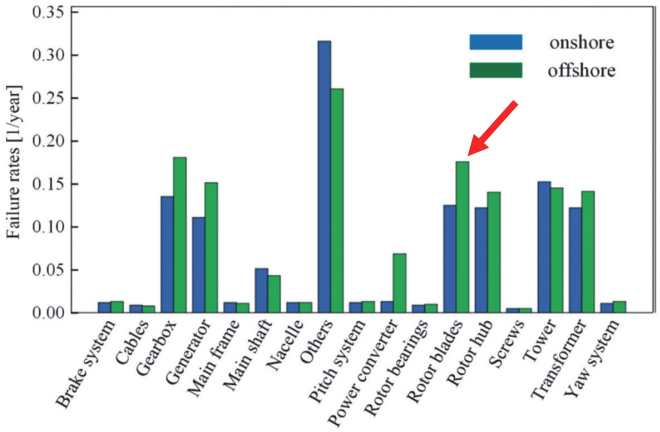

Fig. 1. Failure rates for wind turbine subassemblies working onshore and offshore [Zhu and Li, 2018]

Due to specific sea operating conditions, rotor blades are primarily exposed to intense erosive wear, especially their leading edges (Fig. 2). Due to its nature and intensity, the wear is strictly determined by the wind speed[5], the rotor peripheral speed[6], and the type of particles (their kinetic energy) causing impact loads on the blade profile at the leading edges. Examples of the causes of wear are: rain (hydro-erosion), hail, snow and dust (mechanical erosion) [6]. The damaged surface of the blade's leading edge causes deformation of its profile shape, which generates additional resistance and turbulence. The turboset's rotor then rotates slower and so its generator yields less electricity. However, changes in the mass distribution on the turbine rotor are much more dangerous because they result in imbalance and loss of stability of the entire mechanical system of the wind turboset, the observable symptom of which is resonant vibration being transmitted to its bearing nodes and the supporting structure[7] [4]. This inevitably leads to the dissipation of usable wind energy, as well as accelerated fatigue-wear of the material and structure.

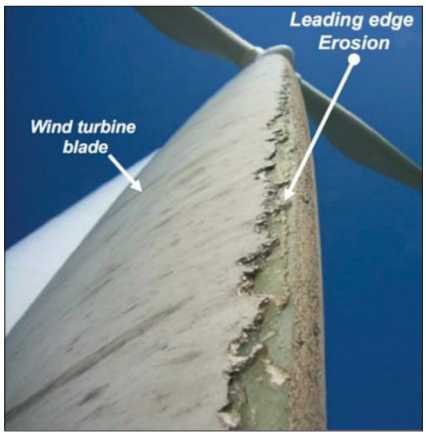

Fig. 2. Eroded leading edge of a wind turbine blade installed in the North Sea after 2 years of operation[8] [https://elektrykapradnietyka.com]

When analysing the physics of the vibrations of a wind turbine rotor, the following causes of their formation should be considered, see Fig. 3 [17]:

- Aerodynamic rotor imbalance (unbalanced aerodynamic forces of the rotor blades F_a). This occurs when, due to erosive wear or icing, one or more rotor blades have a different aerodynamic efficiency (aerodynamic force F_a and also the thrust force F_n) than the others, without a significant change in their masses. This is caused by differences in the aerodynamic aerofoils of individual blades (changes in geometry and shape, as well as increased surface roughness) or deviation of the attack angle of one of the blades from its optimal position, which may happen during operations due to damage to the automatic positioning system. In addition to increased longitudinal (axial) vibrations, an additional consequence of the rotor aerodynamic imbalance is a significant reduction in the effective power of the turbine.
- Rotor mass imbalance (unbalanced centrifugal forces of rotor blades F_r). This occurs when one of the blades is lighter or heavier than the others. In this case, the centre of rotor mass does not coincide with its rotation axis. A significant increase in transverse vibrations occurs, which are transmitted to the entire power train components: main, gear and generator bearings. The imbalance of the rotor mass does not necessarily cause a direct and noticeable loss of the effective power of the turbine (although part of the wind's usable energy is dissipated by forcing vibrations) but the fatigue consequences of cyclic

3 The wind characteristics of most sea areas show that wind turbine sets can operate up to 330 days a year (approximately 8,000 running hours) [12].
4 They increase along with the age of the turboset.
5 100 km/h and more.
6 For example, if the rotor of such a turbine rotates at a rotational speed of 10 rpm, the tip of a 100 m blade moves with a peripheral speed of 105 m/s (377 km/h), and at 30 rpm it would (hypothetically) reach the speed of sound, generating a shock wave.
7 Icing of the rotor blades has a similar effect but this problem is effectively eliminated by an automated blade heating system.
8 In order to minimise the intensity of erosion, additional reinforcements (overlays) are used on the leading edges of the rotor blades, e.g. the manufacturer PolyTech ELLE provides a guaranteed operating time of 15 years.

shock loads on the bearing nodes may significantly shorten the durability of the wind turboset.

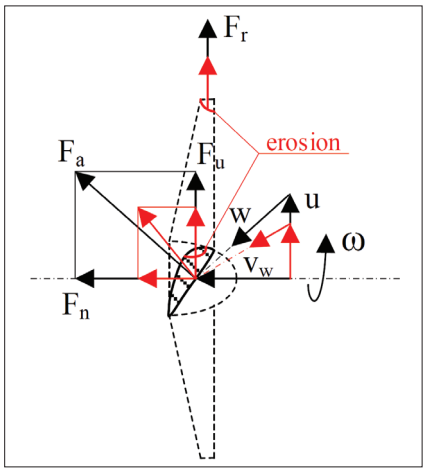

Fig. 3. System of forces acting on the wind turbine rotor blades extorting the rotor to vibrate - red represents alterations in the system corresponding to hypothetical states of aerodynamic and mass instability (imbalance) of the turbine rotor due to blade erosion: F_a – aerodynamic force (lift force), F_n – thrust force (axial), F_u – peripheral force (tangential), F_r – centrifugal force, u – peripheral speed, v_w – wind speed, w – relative speed, ω – rotor angular speed

- Aerodynamic-mass imbalance of the rotor, most often occurring during operations when erosive wear or icing of the rotor blades is associated with a simultaneous and uneven change in the geometry and shape of their profile and mass. Unbalanced aerodynamic forces on the rotor blades intensify the destructive impact of unbalanced inertial (centrifugal) forces F_r originating from unevenly distributed masses performing rotational motion on the rotor structure. An observable symptom is the increased amplitudes of both longitudinal and transverse vibrations transmitted to the bearing nodes of the wind turboset.
- Torsional vibrations in the wind turboset, extorted by the unbalanced peripheral forces of rotor blades F_u, have negligible significance in the case of erosive wear or icing of the rotor blades.

The conclusion is that the early detection of excessive longitudinal and transverse vibrations of the rotor of a wind turboset allows for the elimination of secondary damage to the bearings of its other functional modules (gearbox, generator, drive shafts, and positioning rotor blades). They are usually very extensive, which leads to the immediate shutdown of the entire turboset, resulting in costly maintenance downtime and a need for repairs, see Fig. 3 [7], [9]. For example, the cost of purchasing a planetary gearbox bearing is several thousand euros; however, the cost of replacing it in an offshore wind turboset might be up to several hundred thousand euros, because it must include a service vessel with a crane, disassembly and assembly of the gearbox by a specialised service team, and losses resulting from a long-term interruption in electricity generation [11], [15].

From the numerical data in Fig. 1, it can also be concluded that the gears and generators of offshore (and onshore) wind turbosets are characterised with the same high intensity of damage as rotor blades, the main cause of which are various types of defects in the structural elements of their internal bearings [9].

For the above reasons, the skillful registration of vibration signals generated from bearing nodes, their mathematical processing (determination of diagnostic measures) and, most importantly, their correct interpretation, is a key issue in the diagnostics of offshore wind turbosets [10]. The fundamental metrological question is: "How are the vibrations of the turbine rotor caused by erosion or icing of the rotor blades reflected in the values of the defined diagnostic measures of the bearing nodes of a wind turboset?"

In this way, a set of 'defect-symptom' diagnostic relations is created, which are obtained by appropriate application of the results:

- active experiments – based on the actual introduction of changes in the structure of a model of a wind turbine set built at a small scale (changes in the values of the structural parameters of rotor blades reflect the erosion of their leading edges);
- passive experiments – based on many years of observation of a large number of real tested objects and wind turbine sets of the same type in current operation, without interfering with their structure (technical condition).

In this way, a set of 'defect-symptom' diagnostic relations is created, which are obtained by appropriate usage of the experimental results, as follows:

- active experiments – based on the actual entering of alterations into the structure of a physical model of a wind turboset, built at a small scale (changes in the values of the structural parameters of rotor blades reflecting the erosion or icing of their leading edges);
- passive experiments – based on many years of observation of a large number of real tested objects, wind turbosets of the same type in current operation, without interfering with their structure (technical condition).

These relationships can also be obtained through simulation experiments (numerical) by means of computer programs developed for this purpose – with the possibility of modelling various types of known and recognisable faults to rotor blades. The dynamic development of broadly understood computer software and hardware technology contributes to this, which means that, in recent years, the computer simulation methods of processes have become a very useful tool for designing wind turbosets. There are many works presenting the results of numerical simulations of flow processes in wind turbines for various structural forms and material structures. They were carried out using ANSYS CFD software (ANSYS Fluent, and ANSYS CFX) [1], [14]. It is possible to observe the vibration consequences of turbulence arising on the rotor blade surface as a result of air flow disturbances [3], [5], [14]. However, a significant limitation in their use for diagnostic purposes is the problem of experimental verification of the simulation software. The only way to confirm the reliability of diagnostic simulation experiments is still research carried out on laboratory test beds (small-scale physical models) or, if possible, on a real object, using a measurement system designed on the basis of the results of previously performed numerical simulations of the considered processes.

This was also the main aim of the research undertaken by the authors of this paper. As part of the pilot experimental research program, several measurement cycles of parameters

characterising the basic, and accompanying, processes carried out in the HAWT wind turboset, and constructed at a small scale, were carried out in unbalanced rotor conditions. Vibrations generated from bearing nodes were observed and analysed in terms of the searched diagnostic relations "wind turbine rotor unbalance - vibration diagnostic syndrome of bearing nodes".

RESEARCH METHODOLOGY AND APPLIED MEASURING APPARATUS

Experimental investigations were carried out on a small-scale wind turboset. The schematic diagram and general view of the laboratory test bed are shown in Fig. 4a and 4b. The measurement locations of the observed control parameters are shown in Fig. 5.

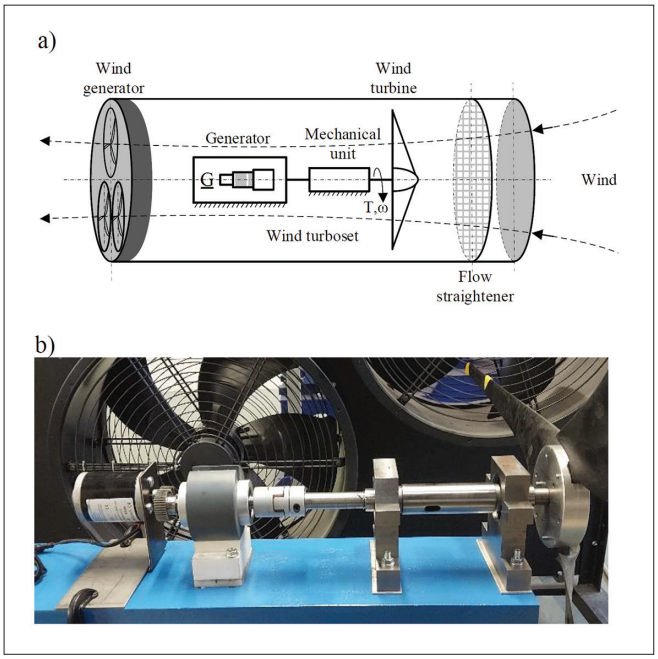

Fig. 4. Laboratory test bed of a small-scale model of the wind turboset: a) schematic diagram, b) general view

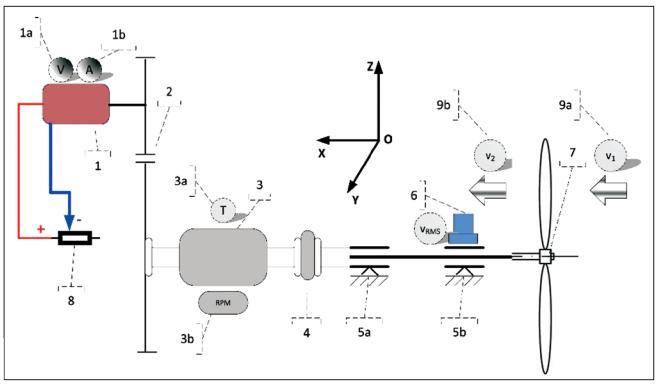

Fig. 5. Measurement points for the observed (monitoring) parameters of the tested wind turboset: 1 – DC generator, 1a – voltage meter, 1b – ampere meter, 2 – 1:1,6 gearbox, 3 – torque meter, 3a - torque measurement, 3b – rotational speed measurement, 4 – flexible coupling, 5a – rear bearing, 5b – front bearing, 6 – triaxial piezoelectric accelerometer, 7 – wind turbine rotor, 8 – power potentiometer, 9a – anemometer on air inlet, 9b – anemometer behind the turbine rotor, v_1 – air velocity in front of the turbine rotor, v_2 – air velocity behind the turbine rotor

The electromechanical unit was placed in a cylindrical channel with a length of 2.5 m and approximately 1.6 m in diameter (see Fig. 6a). An air stream rectifier, consisting of a series of pipes with diameters of 50 mm and lengths of 100 mm (Fig. 6a), was installed in the inlet part of the channel. The air flow in the channel was forced by three axial Ferono FKO600 duct fans (Fig. 4b) equipped with a rotational speed control system. The nominal capacity of each fan was 12,000 m³/h.

In turn, the airflow forces the rotational movement of a three-bladed rotor, with a diameter of 1150 mm, and generates torque transmitted via bearing-mounted, rotating intermediate shafts, a torque meter, and a gear transmission with a ratio of 1:1.6, to a 12V DC generator (Fig. 4b and Fig. 5). The load on the wind turboset was an adjustable resistor, ranging from 0 to 10 Ω (100 W) thereby allowing for changing the operating conditions of the unit.

During the implementation of the research program, continuous measurements of the following monitored parameters were carried out:

- Airspeed before the turbine rotor (v_1) using a thermal anemometer [21]; the position of the measurement probe is shown in Fig. 6a.
- Airspeed after the turbine rotor (v_2) using a second thermal anemometer [21]; the position of the measurement probe is shown in Fig. 6a.
- Torque and rotational speed of the input shaft of the gear transmission [24].
- Vibration acceleration of the front bearing housing [22], [23] (measurement in three axes); the location and view of the accelerometer is shown in Figs. 6a and 6b. The measurement results made it possible to calculate the vibration velocity.
- Voltage at the terminals of the DC generator and current in the generator load circuit [25].

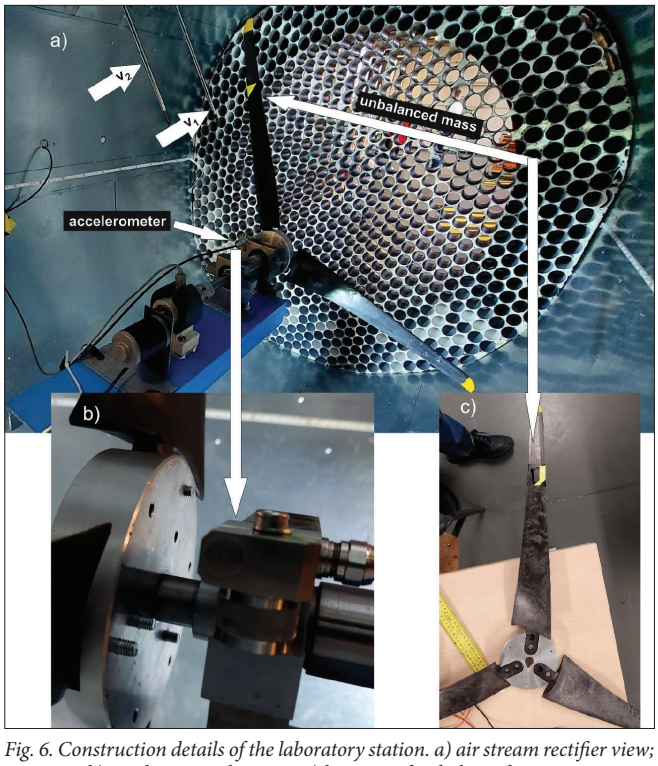

Fig. 6. Construction details of the laboratory station. a) air stream rectifier view; b) accelerometer location; c) location of unbalanced masses

The research was realised in two stages, according to the two respective classes of the technical states of the turboset:

- Useful, reference state (ref.): the wind turboset without any modifications to the technical condition of individual elements.
- Unserviceable state (F1): a modification involving the introduction of imbalance by adding extra mass mw, attached to one of the rotor blades, as shown in Figs. 6a and 6c ($m_w = 4g$, $m_w = 4g \rightarrow 2\%$ of the rotor blade mass, 0.3% of the total rotor mass).

In each state, four measurement points were selected, defined by the load value of the generator, realised using an adjustable resistor. The current-voltage parameters were adjusted to the existing operational limitations of the laboratory station, see Fig. 7 and Fig. 8.

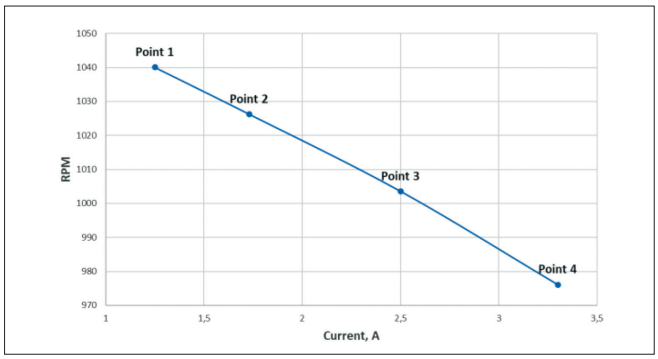

Fig. 7. The values of the generator load current I and the corresponding wind turboset rotor speed values n, during the tests for the selected measurement points

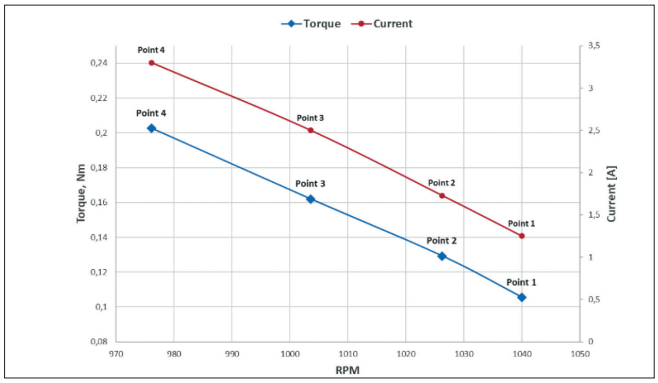

Fig. 8. The values of torque and rotational speed (T, n) measured at the input of the gear transmission

The sets of variables subject to measurements (calculations) were determined as follows (Fig. 4b, Fig. 5):

Input variables:

- The capacity of the wind generator fans corresponding to a specific setting of the speed regulator of the electric drive motors (the nominal inverter setting value $h_{inv} = 300$, resulting in fan rotor speeds of approximately 80% of the nominal rotational speed).
- Generator load current – I.
- Airspeed at the turbine rotor inlet – v_1.
- Airspeed after the turbine rotor – v_2.
- Voltage at the generator terminals – U.
- Generator power – P_{el}.
- Rotational speed of the turbine rotor – n.
- Torque at the input of the gear transmission – T.
- RMS (*Root Mean Square*) values of vibration velocities determined in the horizontal plane: OX axis – longitudinal vibrations, OY axis – transverse vibrations and in the vertical plane, OZ axis - transverse vibrations.

The crest factor CF – defined as:

$$CF = \frac{a_{Peak}}{a_{RMS}} \quad (1)$$

where:

- a_{Peak} – peak value of vibration acceleration, m/s²;
- a_{RMS} – RMS value of vibration acceleration, m/s².

RESULTS AND DISCUSSION

As a result of the vibration acceleration measurements and the corresponding calculations of vibration velocities, the following results were obtained.

- RMS of the vibration velocity – as a measure of kinetic energy dissipation in the rotation of a wind turbine set.

Tab. 1. Obtained RMS results of the vibration velocity $v_{RMS_{OX}}$, $v_{RMS_{OY}}$, $v_{RMS_{OZ}}$

Axes	Measure point:	State ref.		State F1		Deviations	
		v_{RMS}	CF	v_{RMS}	CF	δv_{RMS}	δCF
		mm/s	–	mm/s	–	–	–
OX	1	3.33	3.54	6.76	3.60	103%↑	2%↑
	2	3.35	3.52	8.92	2.68	166%↑	-24%↓
	3	3.28	3.61	8.31	3.42	153%↑	-5%↓
	4	3.09	3.61	10.2	2.84	230%↑	-21%↓
OY	1	1.73	5.62	16.8	2.24	871%↑	-60%↓
	2	1.71	5.00	17.0	2.24	894%↑	-55%↓
	3	1.54	6.38	16.5	2.41	971%↑	-62%↓
	4	1.72	4.76	16.6	2.50	865%↑	-47%↓
OZ	1	2.56	3.85	25.2	2.30	884%↑	-40%↓
	2	2.49	4.06	25.6	2.36	928%↑	-42%↓
	3	2.47	3.84	25.1	2.40	916%↑	-38%↓
	4	2.78	4.34	22.6	2.67	713%↑	-38%↓

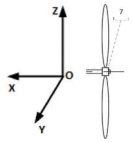

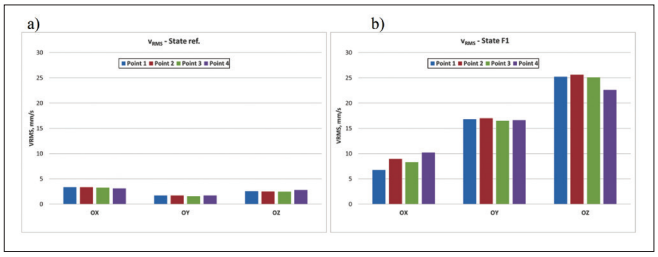

Fig. 9. Summary of the resulting values for each measurement point in: a) state ref., b) state F1

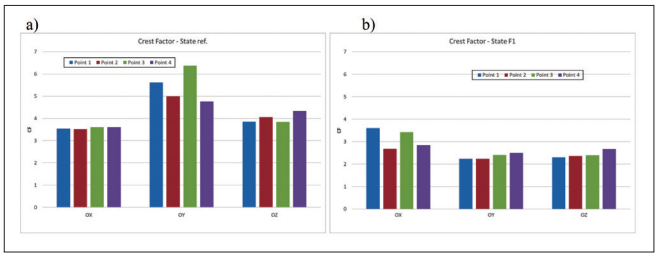

Fig. 10. Summary of the resulting crest factor values (CF) for each measurement point in a) state ref., b) – state F1

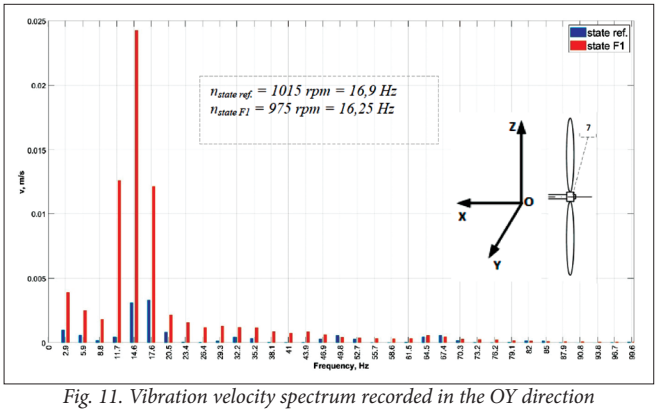

Fig. 11. Vibration velocity spectrum recorded in the OY direction

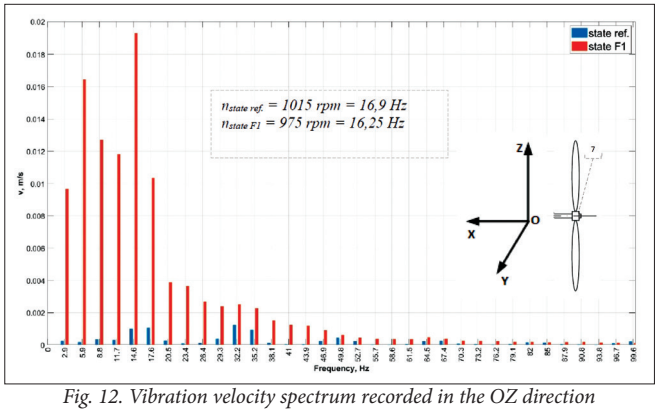

Fig. 12. Vibration velocity spectrum recorded in the OZ direction

• Spectral analysis – to identify potential sources of generated vibrations.

In addition, the results obtained for all measurement points were subjected to spectral analysis. Forced transverse and longitudinal vibrations occur in wind turbine units, practically across the entire range of rotational speed variations, but their largest amplitudes arise at resonant rotational speeds. To identify the sources of resonance, a spectral analysis of the recorded vibration signals must be conducted, which involves decomposing it into harmonic components at specific resonant frequencies. The concentration of the amplitude spectrum and the increase in amplitudes of characteristic harmonic components indicate the occurrence of local resonances and the deterioration of the dynamic state of the wind turbine unit. This is associated with the risk of secondary fatigue damage to the elements transmitting torque from the wind turbine rotor to the generator, such as bearing nodes.

Due to the extensiveness of the obtained material, only a part of the results is presented here, concerning the results of vibration measurement in the OY and OZ directions for the maximum value of the generator load, at measurement point 4. Despite the partial nature of the presented results, they present certain regularities that could be determined on the basis of the experiments.

The frequency analysis of the recorded amplitude spectra of vibration velocity generated from the front bearing of the wind turbine rotor drive shaft, with the highest effective values, showed that all analysed vibration velocity spectra exhibit clear concentrations of harmonic components near the fundamental frequencies of the rotor drive shaft's rotations. These harmonic components are the main sources of vibration excitation in the radial direction, due to mass unbalancing in the rotor's rotational movement.

At the same time, it is essential to consider the mechanical characteristics of the applied flexible coupling, which significantly alters the dynamic parameters of the entire drive line. The purpose of this is to detune the resonances and reduce the stress induced by vibrations in the torque-transmitting elements.

• Drive characteristics – for evaluating the efficiency of energy transformation processes carried out in the wind turboset.

Based on the mechanical, electrical and aerodynamic monitoring parameters of the wind turboset, registered in two different dynamic states of the turbine rotor (the reference (ref.) and aerodynamic-mass imbalance (F1)), its basic parameters and rotational speed characteristics (drive characteristics) were determined, see Figs. 13 and 14. This made it possible to perform a qualitative and quantitative analysis of the impact of the actually entered rotor imbalance (alterations in structural parameters) on the energy state of the entire wind turboset.

• The numerical data on the air flow speed variability characteristics before v_1 and after the rotor v_2 of the wind turbine (Fig. 13) show that, with the increase in the load on the electric generator while maintaining the set (constant) capacity of the wind generator, the rotational speed of the turboset decreases (the kinetic energy of the rotating masses decreases), which is also reflected in the increase in wind speed in the turbine inlet section (its kinetic energy increases), see Fig. 13a. The rotor imbalance entered resulted in a slight (3-4%) decrease in the speed v_1 and the kinetic energy of the wind in the turbine inlet cross-section. However, despite a

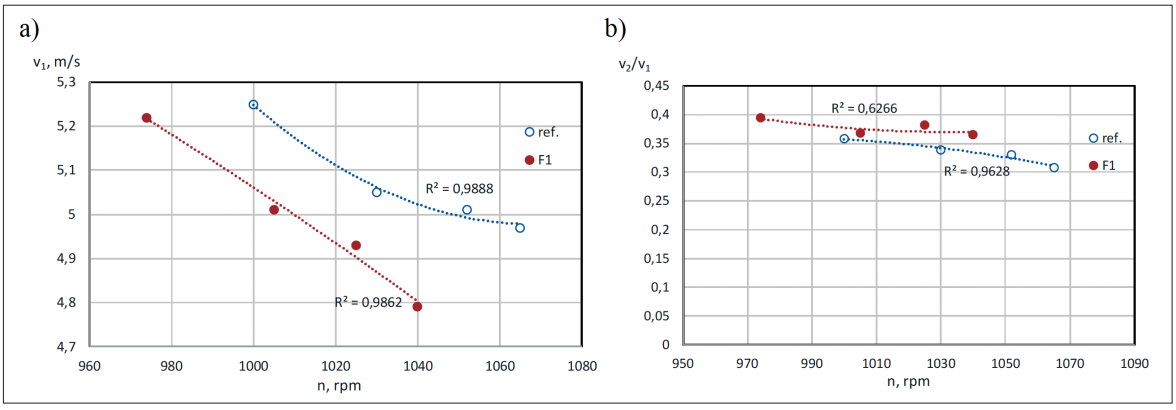

Fig. 13. Courses of the air flow velocity in the inlet cross-section of the turbine rotor v_1 (a) and the air flow velocity ratio in the outlet and inlet cross-section of the turbine rotor v_2/v_1, respectively (b), in terms of the rotor rotational speed n for two dynamic states of the wind turboset: ref. and F1

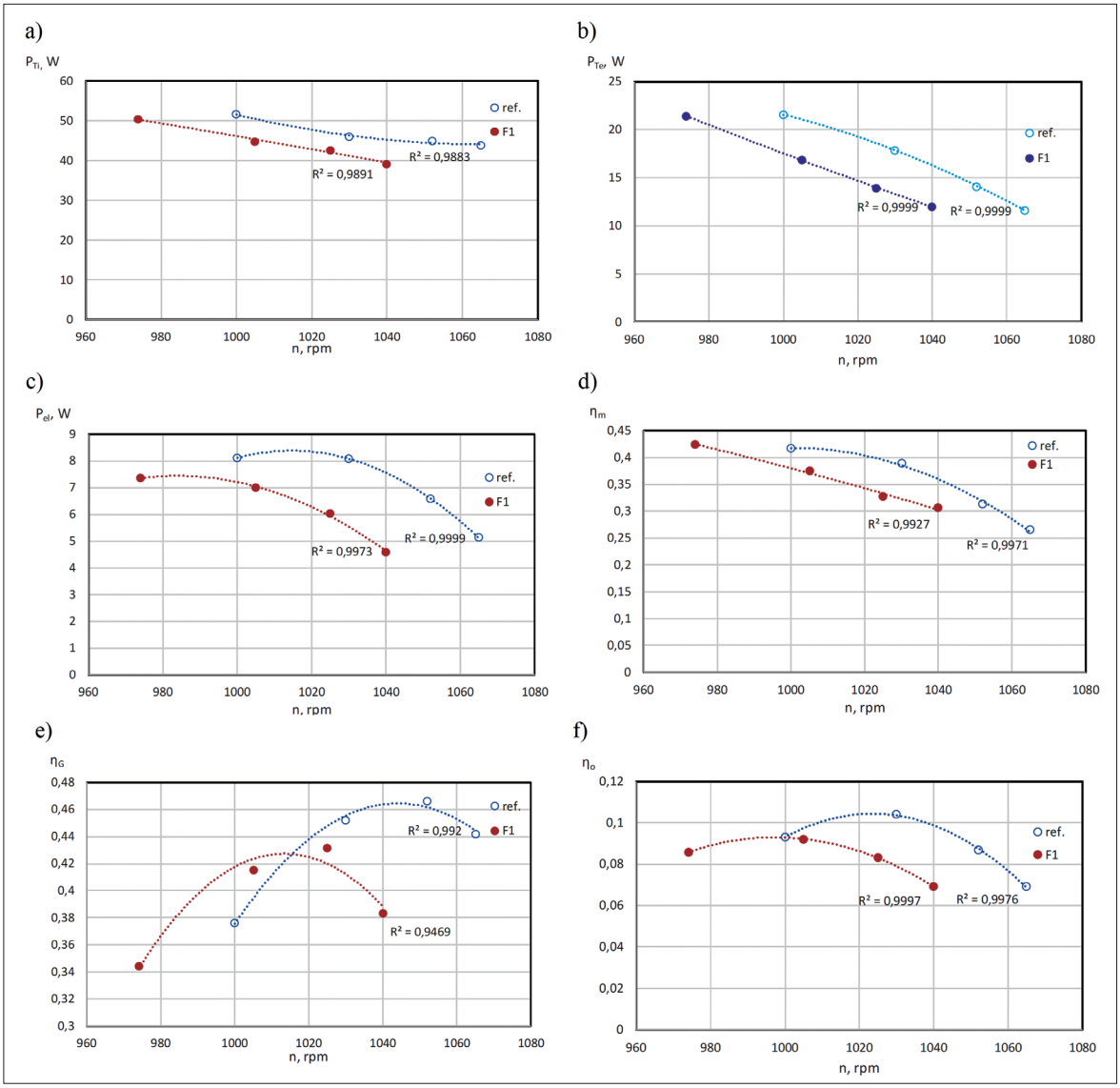

Fig. 14. Courses of the internal power of the turbine P_{Ti} (a), the effective power of the turbine P_{Te} (b), the power at the electric generator terminals P_{el} (c), the mechanical efficiency of the wind turboset η_m (d), the efficiency of the electric generator η_G (e), and the overall efficiency of the wind turboset η_o (f), in terms of the rotor rotational speed n, for two dynamic states of the wind turboset: ref. and F1

noticeable increase of almost 10% in the ratio of air flow speed through the turbine v_2/v_1 (up to 0.4), as shown in Fig. 13b, the relative decrease in the aerodynamic efficiency of the turbine $\delta\eta_a$ was insignificant, not exceeding 1%.

- By comparing the numerical data on the generated power variability characteristics in Fig. 14a-c, it can be concluded that, due to the imbalance of the turbine rotor, the performance of the turboset decreased significantly. The relative decrease in the generated internal power of the turbine δP_{Ti} is more than 10%, the decrease in turbine effective power δP_{Te} is more than 20% and, for the power at the terminals of the electric generator δP_{el}, the reduction reaches 25%.
- In turn, when comparing the efficiency characteristics of the implemented transformation processes of various forms of energy in the turboset, the electric generator efficiency η_G responded most strongly to the turbine rotor imbalance, the relative value of which decreased by approximately 17% (Fig. 14e). Then, the mechanical efficiency of the turboset $\delta\eta_m$ decreased by approximately 12% (Fig. 14d). The total relative drop in the overall efficiency of the wind turboset $\delta\eta o$, due to imbalance (after taking into account a 1% decrease in aerodynamic efficiency $\delta\eta a$), is approximately 30% (Fig. 14f).

FINAL REMARKS AND CONCLUSIONS

Simultaneous measurements of longitudinal and transverse vibrations, generated from the front bearing of the wind turbine's rotor drive shaft, as well as control measurements of the mechanical, electrical, and aerodynamic parameters characterising the load condition of the wind turbine unit, provide the possibility of determining a generalised imbalance syndrome of the turbine rotor, regardless of its nature, in the following form: $\{SF1\} = \{\delta v_{RMS}, \delta CF, \delta P_{Te}\}$. The symptoms of rotor imbalance are the relative deviations of the following diagnostic parameters: root mean square velocity of vibrations

(v_{RMS}), crest factor (CF), and effective power of the wind turbine (P_{Te}).

The results of the active experiments conducted showed that a significant element in assessing the dynamic state of the wind turbine is the spectral-correlation analysis of the recorded vibration signal generated from the front bearing of the drive shaft. The attractiveness of spectral analysis is confirmed by its widespread use in the diagnostics of full-size wind turbine units, as it allows the tracking of the trend of changes in the spectrum parameter values in various characteristic frequency bands during operations, under known and recognisable states of rotor imbalance.

As a result of the aerodynamic-mass imbalance actually introduced into the physical model of the wind turbine unit, the largest (almost tenfold) increase in the root mean square value of transverse vibration velocity was observed, both on the vertical (OZ) and horizontal (OY) axes, with only a twofold increase in the root mean square value of longitudinal vibration velocity (on the OX axis). Since this was not accompanied by a noticeable decrease in the aerodynamic efficiency of the turbine, it can be concluded that the dominant destructive factor was the unbalanced centrifugal forces of the rotor blades, with their unbalanced thrust forces playing a significantly smaller role.

REFERENCES

1. Bekhti A, Guerri O, Rezoug T. Numerical simulation of fluid flow around free vibrating wind turbine airfoil. Proceedings of the International Conference on Numerical Analysis and Applied Mathematics, Rhodes, 1648(1), 850088, 2015. https://doi.org/10.1063/1.4913143.

2. Buljan A. Offshore Wind Turbines in 2023. January 2, 2024. https://www.offshorewind.biz, accessed on 2024-05-10.

3. Hansen MH. Improved modal dynamics of wind turbines to avoid stall-induced vibrations. Wind Energy, vol. 6, pp. 179-195, 2003. https://doi.org/10.1002/we.79.

4. Hu WH, Thöns S, Rohrmann RG, Said S. Vibration-based structural health monitoring of a wind turbine system. Part I: Resonance phenomenon. Engineering Structures vol. 89: pp. 260–272, 2015. https://doi.org/ 10.1016/j.engstruct.2014.12.034.

5. Jureczko M, Pawlak M, Mezyk A. Optimisation of wind turbine blades. Journal of Materials Processing Technology, vol. 167, (2-3): pp. 463–471, 2005. https://doi.org/10.1016/j.jmatprotec.2005.06.055.

6. Katsaprakakis DA, Nikos P, Ioannis N. A comprehensive analysis of wind turbine blade damage. Energies, vol. 14, (18), 5974, 2021. https://doi.org/.10.3390/en14185974.

7. Lau BCP, Ma EWM, Pecht M. Review of offshore wind turbine failures and fault prognosis methods. Proceedings of 3rd Annual Prognostics and System Health Management Conference, PHM-2012, Beijing, China, 23-25 May 2012, 2012. https://doi.org/ 10.1109/PHM.2012.6228954.

8. Letcher TM. Wind Energy Engineering. A Handbook for Onshore and Offshore Wind Turbines. Academic Press. Elsevier Inc. 2017.

9. Liu Z., Zhang L. A review of failure modes, condition monitoring and fault diagnosis methods for large-scale wind turbine bearings. Measurement, vol. 149, 107002, 2020. https://doi.org/ 10.1016/j.measurement.2019.107002.

10. Márquez GFP, Tobias AM, Pérez JMP, Papaelias M. Condition monitoring of wind turbines: Techniques and methods. Renewable Energy, vol. 46, pp. 169-178, 2012. https://doi.org/10.1016/j.renene.2012.03.003.

11. Mcmillan D, Ault GW. Quantification of Condition Monitoring Benefit for Offshore Wind Turbines. Wind Engineering, vol. 31(4), pp. 267-285, 2007. https://doi.org/10.1260/030952407783123060.

12. Passon P. Offshore Wind Turbine Foundation Design. Dissertation. Technical University of Denmark, Department of Wind Energy, 2015.

13. Sellami T et al. Modal and harmonic analysis of three-dimensional wind turbine models. Wind engineering, vol. 40, (6), pp. 518-527, 2016a. https://doi.org/10.1177/0309524X16671093.

14. Sellami T. et al. Original numerical analysis of wind turbine vibration. The 7th International Renewable Energy Congress, Hammamet, Tunisie, IREC 2016, 22-24 March 2016, 2016b.

15. Spinato F. The Reliability of Wind Turbines. Dissertation, Durham University, UK, 2008.

16. Walford C. Wind Turbine Reliability: Understanding and Minimizing Wind Turbine Operation and Maintenance Costs. Sandia National Laboratories, Rep. SAND-2006-1100. 2006. https://doi.org/10.2172/882048.

17. Wu B, Lang Y, Zargari N, Kouro S. Power Conversion and Control of Wind Energy. John Wiley & Sons, INC., Publication, 2011. https://doi.org/10.1002/9781118029008.

18. Zhu C, Li Y. Stability Control and Reliable Performance of Wind Turbines. Chapter 9: Reliability Analysis of Wind Turbines. Edited by Kenneth Eloghene Okedu, IntechOpen, 2018. https://doi.org/ 10.5772/intechopen.74859.

19. ISO 10816-21:2015 Mechanical vibration - Evaluation of machine vibration by measurements on non-rotating parts. Part 21: Horizontal axis wind turbines with gearbox, 2015.

20. https://elektrykapradnietyka.com. Offshore wind turbine blades after 2 years of service in the North Sea, accessed on 2024-05-10.

21. https://benetech-poland.pl/anemometry-wiatromierze/62-termo-anemometr-hot-wire-benetech-gm-8903-5903738810338.html, accessed on 2024-05-10.

22. https://svantek.com/products/svan-958a-four-channels-sound-vibration-meter/, accessed on 2024-05-14.

23. https://svantek.com/accessories/sv-85-triaxial-outdoor-accelerometer-100-mv-g-connector-m12-m6-mounting-hole/, accessed on 2024-05-14.

24. http://www.momentomierze.pl/momentomierze.html, accessed on 2024-06-10.

25. https://www.egsystem-sklep.pl/multimetr-bm857s-trmsac-ad-brymen-p-4779.html, accessed on 2024-05-10.

26. https://svantek.com/softwares/svanpc-software/, accessed on 2024-05-14.